Electrical power generator from randomly oriented electrospun poly(vinylidene fluoride) nanofibre membranes

AUTHOR(S)

Jian Fang, Xungai Wang, Tong Lin

COMMUNICATION

Electrical power generator from randomly oriented electrospun poly(vinylidene fluoride) nanofibre membranes†

Jian Fang, Xungai Wang and Tong Lin*

Randomly oriented electrospun poly(vinylidene fluoride) nanofibre membranes were directly used as active layers to make mechanical-to-electrical energy conversion devices. Without any extra poling treatment, the device can generate voltage outputs as high as several volts upon receiving a mechanical impact. The device also showed long-term working stability and the ability to drive electronic devices.

The recent boom in miniature electronic devices has raised concerns about their working sustainability.[1,2] Because of the large number, small dimensions and complicated application environments (*e.g.* inside a biological or human body, underground or in remote areas), powering these devices with conventional batteries meets difficulties in replacement or on-site charging of the batteries.[3] Self-powering of electronic devices by integrating a power generator that can scavenge and turn the surrounding local energy (*e.g.* mechanical, thermal or chemical) into electrical energy to drive the electronic devices sustainably without any other electrical input has emerged as a viable solution. Piezoelectric harvesting of mechanical energies using inorganic semiconductive nanowires (from ZnO,[4] InN,[5] GaN,[6] CdS[7] and ZnS[8]) has received great attention, since the first report on using ZnO nanowires for electrical generation in 2006.[4] These nanowire-based electrical generators have shown the ability to harvest mechanical energy from body movements, acoustic/ultrasonic vibrations or hydraulic forces into electrical energy,[9,10] which could be a promising candidate for adding self-powering features to miniature electronics.

The inorganic nanowire-based electrical generators, however, require precisely controlled fabricating conditions. They are brittle and have a very limited strain level. Despite the wide working frequency range, the devices have to work under very small forces to avoid damage to the nanowires inside. Consequently, these devices are typically low in power output. The brittle inorganic nanowires are also difficult to integrate into flexible substrates.

Polymer nanofibres have much better flexibility than inorganic nanowires. They are mostly produced by electrostatic spinning technology in which a polymer solution is rapidly stretched under a strong electrical field to form dry fibres with the diameter controllable in the range between a few nanometres to several micrometres.[11] Depending on the fibre collection methods used, either randomly oriented nonwoven mats or aligned nanofibres can be produced. Recently, single poly(vinylidene fluoride) (PVDF) nanofibre prepared by a near field electrospinning technique and aligned PVDF nanofibres produced by a conventional electrospinning method have been used separately in piezoelectric power generators.[12,13] The near field electrospun PVDF nanofibre was directly used for making power generators without additional poling treatment, and the device generated electricity upon lateral stretching.[12] In contrast, the aligned PVDF nanofibres required a post-electrospinning poling treatment to make the molecular dipole of the polymer orient along the fibre length direction.[13]

In our recent experiment, we have found that randomly oriented electrospun nanofibre membrane can be directly used to prepare a piezoelectric power generator without any extra poling treatment. The power generator device can be prepared simply by sandwiching an as-spun PVDF nonwoven membrane between two metal foils. The electrical output can be as high as several volts. Herein, we report on the mechanical-to-electrical energy conversion of the novel nanofibre power generation devices.

Fig. 1a illustrates the electrospinning setup for making PVDF nanofibre membranes. The morphology of the as-spun PVDF nanofibres is shown in Fig. 1b. Randomly oriented fibres with an average diameter of 183 ± 37 nm were collected. The nanofibres revealed a rough surface (see inset image in Fig. 1b). The Fourier Transform Infrared (FTIR) spectrum of the as-spun nanofibre membrane shows strong vibration peaks at 840 cm^{-1} and 1280 cm^{-1} (Fig. 1c), which are typical vibration characteristics of the β crystalline phase. The β phase was confirmed by the X-ray diffraction (XRD) data which had a strong β phase crystalline signal with 2θ at 20.5° (Fig. 1d). For comparison, the FTIR and XRD results of PVDF cast film are also shown in Fig. 1c and 1d. It is clearly revealed that the cast film has a much weaker β phase. This suggests that electrospinning favours the formation of β phase crystalline PVDF.

Fig. 2a illustrates the schematic of the energy conversion device, which consisted of a PVDF nanofibre membrane (thickness 140 μm) and two aluminium foil electrodes. The metal electrodes were attached separately to the two sides of the nanofibre membrane. An electrochemistry working station (e-corder 401) was used to collect the electrical signals. Upon rapidly compressing the device from one side, pulse voltage outputs were detected. Fig. 2b shows typical

Centre for Material and Fibre Innovation, Deakin University, Geelong, VIC 3217, Australia. E-mail: tong.lin@deakin.edu.au
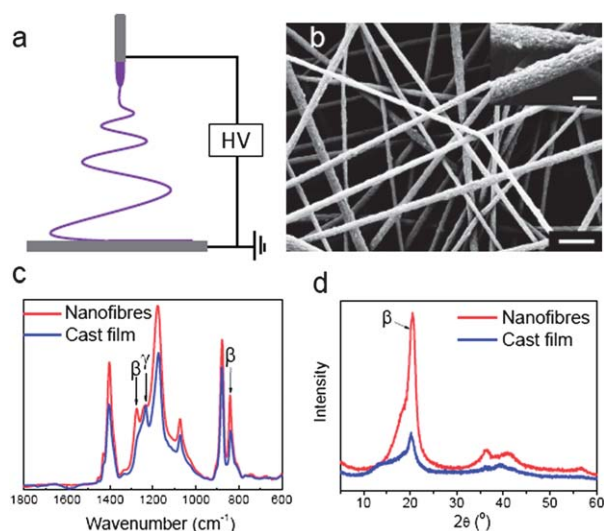
Fig. 1 a) Electrospinning setup. b) SEM images of electrospun PVDF nanofibres (scale bar: 1 μm, inset scale bar: 200 nm). c) FTIR spectra of electrospun PVDF nanofibre membrane and PVDF cast film. d) XRD patterns of electrospun PVDF nanofibre membrane and PVDF cast film.
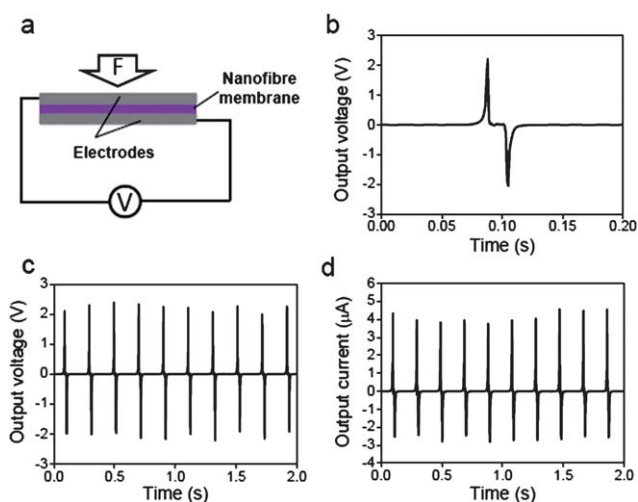

Fig. 2 a) Illustration of power generating device. b) Typical voltage outputs of a nanofibre membrane device subjected to an impact action (initial impact speed, 34 mm s^{-1}). c) Voltage and d) current outputs of the same nanofibre device under 5 Hz repeated compressive impacts. Nanofibre membrane thickness = 140 μm; working area = 2 cm^2.

voltage outputs of a nanofibre device. When the device was subjected to a compression and then release impact, a pulse voltage signal accompanied with an opposite pulse voltage output was recorded. The first signal (referred to as "front output") was derived from the compressive deformation of nanofibres within the membrane, while the subsequent opposite output (referred to as "back output") was attributed to the recovery deformation of the compressed nanofibres due to the release of the impact force. To verify this, the device was just impacted and the compressed state was then held instantly, without releasing the force. In this case, only the front output signal was collected but not the back output (see ESI†).

Upon repetitively impacting the nanofibre membrane device, the pulse voltage outputs occurred constantly. Fig. 2c and d show the

voltage and current outputs of the nanofibre membrane device subjected to 5 Hz repeated compressive impact-and-release cycles. The outputs were stable and the time interval between the neighbouring same-polarity pulses matched well with the impact frequency.

The polarity of the electrical outputs was found to be determined by the device side that received the compressive impact and the way to connect with the electrochemistry working station. When the electrode that received the compressive impact was connected to the counter electrode, while the opposite electrode was connected with the working electrode, a positive front output voltage followed by a negative back output was always detected for an impact-and-release cycle. However, when the connection was reversed, the voltage and current outputs reversed the polarity (see ESI†). These results suggest that the negative electrode of the nanofibre device is always associated with the device side that directly receives the impact force.

Impact frequency showed a considerable effect on the electrical output. As shown in Fig. 3a, under the 1 Hz compressive impacts, the average peak voltage output is 0.43 V. When the impact frequency was increased to 5 Hz, the voltage output became 2.21 V. Further increasing the frequency to 10 Hz led to the output voltage reaching up to 6.3 V (Fig. 3b). With the increase in the working frequency, more uneven output signals were recorded, presumably due to the incomplete recovery of fibres from the compressive deformation, or the mechanical vibration from the pressing device itself. The frequency-dependent electrical output originates from the influence of initial impact speed. For the impact frequency of 1, 5, and 10 Hz, the initial impact speed is 6.8, 34 and 68 mm s^{-1}, respectively. Such a high voltage generated by a low initial impact speed is beneficial in harvesting electrical energy from movements of the human body.[1,14]

The duration for the occurrence of the back output was also affected by the impact speed. As also shown in Fig. 3b, with an increase in the impact speed, the occurrence of the back output takes a shorter period of time. When the impact frequency was 1 Hz, which equals an initial impact speed of 6.8 mm s^{-1}, the recovery signal peak occurred 0.111 s after the front output. When the initial impact speed was increased to 34 and 68 mm s^{-1}, the occurrence of the back output was delayed to 0.017 and 0.01 s, respectively.

For comparison, a commercial piezoelectric PVDF film (Measurement Specialties, USA) was also subjected to the same compressive impact, and the voltage output was about 0.32 V (see ESI†), despite the fact that the film has a strong piezoelectric response to bending. The relatively low compressive piezoelectric response is probably because of the dense structure of the PVDF film, which is
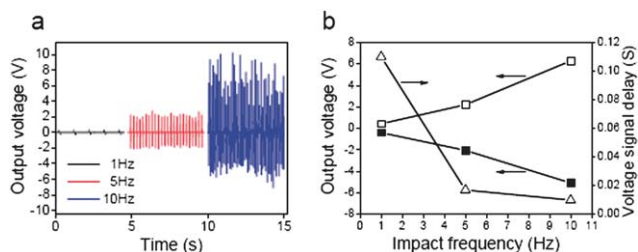

Fig. 3 a) Voltage outputs of a nanofibre device under different impact frequencies. b) Dependences of output voltages and delay time of the opposite voltage on impact frequency. □: positive voltage outputs, ■: negative voltage outputs, △: voltage signal delay. Membrane thickness = 140 μm; working area = 2 cm^2.

less deformed by the compressive impact compared to the highly porous nanofibrous membrane.

As with a dense piezoelectric PVDF film, the mechanical-to-electrical energy conversion stems from the crystalline β phase of the polymer and oriented molecular dipoles within the film,[15] which is difficult to obtain directly from a film-making process, and conventionally a poling treatment has to be used to achieve this.[16] The molecular dipole after poling is in the same direction within the film.

For our nanofibrous devices, the power was generated although the nanofibre membranes were not poled after electrospinning. This suggests that electrospinning assists in forming oriented molecular dipoles within nanofibres, besides the formation of a high β phase. We also found that when two metal electrodes were added to the same side of a nanofibre membrane, but leaving a small gap between them, no piezoelectric responsiveness was detected no matter how the membrane was impacted mechanically. It is therefore important to add the metal electrodes to the two opposite sides of the nanofibre membrane for the electrical generation. However, the fact that the output polarity is impact-side-dependent suggests the molecular dipoles within nanofibres are unlikely to orient along the fibre length direction. This was confirmed by Hansen et al.'s study[13] that when aligned electrospun PVDF nanofibres were used to make power generation devices, a post-electrospinning poling treatment had to be used to make the molecular dipoles align along the fibre length direction.

It should also be pointed out that our nanofibre power generating device differs substantially from the nanofibre nanogenerator reported by Chang et al.[17] In their nanogenerators, the device was made of a short single fibre prepared by a direct-write electrospinning technique, and the piezoelectric power was generated along the fibre length direction, therefore the molecular dipoles should align along the fibre length direction. In our case, the power generating device was made of continuous fibres having a randomly oriented nonwoven structure, and the piezoelectric power was generated across the web thickness, which was in the direction perpendicular to the fibre length. However, the actual power generation mechanism of our nanofibre membrane generator is not clear, thus warranting further study.

To convert the voltage outputs to DC signals, a full wave rectifier bridge was used (Fig. 4a) and the rectified voltage output reached 1.25 V (Fig. 4b), despite the energy consumption in the diodes (the rectified current output is shown in ESI†). Fig. 4c shows the voltag–charging time relationship of the nanofibre device. Under the same impact frequency (5 Hz), the charging speed for different capacitors varied. It took less than 2 min to charge a 2.2 μF capacitor to over 3 V, and the time needed to charge a 33 μF capacitor to light up a commercial blue LED was about 30 min. When a 200 kΩ resistor was used to stabilise the output voltage, the one-time charged capacitor could light the LED for over 20 s before complete consumption of the power, as illustrated in Fig. 4d (the video is given in ESI†). Also, the nanofibre power generator can work over a long period of time without any performance surrender. Stable outputs have been recorded over one hour of continuous compression (see ESI†).

For the previously reported nanowire and PVDF nanofibre power generators,[4,10,17] the voltage outputs are mostly very low, typically around tens of millivolts. To increase the voltage output level, an integrated nanogenerator composed of hundreds of power generating
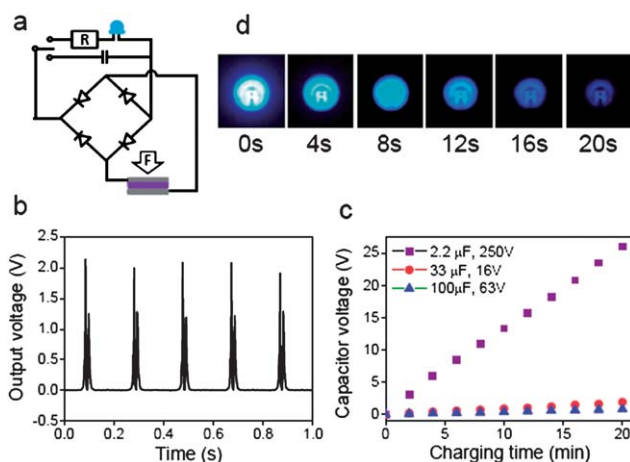

Fig. 4 a) Circuit for charging a capacitor and lighting a LED device. b) DC voltage output rectified from a nanofibre membrane device. c) Voltage–charging time relationship for a nanofibre membrane device loaded with different capacitors. d) Still frames captured from a video showing continuous lighting of a blue LED powered by a nanofibre power generator. Working area = 2 cm²; thickness = 140 μm; impact frequency = 5 Hz.

units has to be used. A peak voltage of 1.26 V was achieved only recently,[18] but the preparation was very complicated. It took 120 min for a ZnO nanowire device (1 cm²) to charge a 2.2 μF capacitor to 0.37 V, and a commercial LED was lit up for only 0.1–0.2 s when ten such device–capacitor couples were used in parallel.[19]

The maximum energy conversion efficiency (η_{max}) of the piezoelectric nanofibre membrane can be calculated from the electrical power (W_e) generated from the mechanical energy (W_m) transferred onto the membrane.

$$\eta_{max} = W_e/W_m$$

W_e can be calculated as:

$$W_e = \int VI \, dt$$

where V and I are the voltage and current measured. The mechanical energy can be calculated using an indirect method (for details see ESI†). The estimated conversion efficiency of a 2 cm² nanofibre membrane device at 1 Hz, 5 Hz and 10 Hz compression frequencies was 7.89%, 8.01% and 13.62%, respectively. The impact frequency also affected the energy conversion efficiency.

Apart from the compressive impact, other mechanical movements, such as bending and tapping, were also able to induce electrical output (see ESI†). Detailed and systematic results from optimised device structure will be reported in the near future.

Conclusions

We have demonstrated a one-step fabrication of piezoelectric PVDF nanofibre membrane that can be used to convert mechanical energy to electrical power. High voltage outputs were obtained and the electrical energy was able to be stored to power electronic devices. This nanofibre membrane power generating device may provide a simple, efficient, cost-effective and flexible solution to self-powering of microelectronics for various purposes.

Notes and references

1 Z. L. Wang, *Sci. Am.*, 2008, 82–87.
2 Z. L. Wang, *Tech. Dig.-Int. Electron Devices Meet.*, 2007, 371–374; R. Bogue, *Sens. Rev.*, 2010, **30**, 182–186; R. Bogue, *Sens. Rev.*, 2010, **30**, 271–275.
3 Z. L. Wang, *Nano Today*, 2010, **5**, 512–514.
4 Z. L. Wang and J. Song, *Science*, 2006, **312**, 243–246.
5 C. T. Huang, J. Song, C. M. Tsai, W. F. Lee, D. H. Lien, Z. Gao, Y. Hao, L. J. Chen and Z. L. Wang, *Adv. Mater.*, 2010, **22**, 4008–4013.
6 C. T. Huang, J. Song, W. F. Lee, Y. Ding, Z. Gao, Y. Hao, L. J. Chen and Z. L. Wang, *J. Am. Chem. Soc.*, 2010, **132**, 4766–4771.
7 Y. F. Lin, J. Song, Y. Ding, S. Y. Lu and Z. L. Wang, *Adv. Mater.*, 2008, **20**, 3127–3130; Y. F. Lin, J. Song, Y. Ding, S. Y. Lu and Z. L. Wang, *Appl. Phys. Lett.*, 2008, **92**, 022105.
8 M.-Y. Lu, J. Song, M.-P. Lu, C.-Y. Lee, L.-J. Chen and Z. L. Wang, *ACS Nano*, 2009, **3**, 357–362.
9 X. Wang, J. Liu, J. Song and Z. L. Wang, *Nano Lett.*, 2007, **7**, 2475–2479; X. Wang, Y. Gao, Y. Wei and Z. L. Wang, *Nano Res.*, 2009, **2**, 177–182; R. Yang, Y. Qin, C. Li, G. Zhu and Z. L. Wang, *Nano Lett.*, 2009, **9**, 1201–1205; Z. Li, G. Zhu, R. Yang, A. C. Wang and Z. L. Wang, *Adv. Mater.*, 2010, **22**, 2534–2537.
10 X. Wang, J. Song, J. Liu and Z. L. Wang, *Science*, 2007, **316**, 102–105.
11 D. Li and Y. Xia, *Adv. Mater.*, 2004, **16**, 1151–1170; A. Greiner and J. H. Wendorff, *Angew. Chem., Int. Ed.*, 2007, **46**, 5670–5703; T. Lin, H. Wang and X. Wang, *Adv. Mater.*, 2005, **17**, 2699–2703; J. Fang, H. Niu, T. Lin and X. Wang, *Chin. Sci. Bull.*, 2008, **53**, 2265–2286.
12 C. Chang, V. H. Tran, J. Wang, Y. K. Fuh and L. Lin, *Nano Lett.*, 2010, **10**, 726–731.
13 B. J. Hansen, Y. Liu, R. Yang and Z. L. Wang, *ACS Nano*, 2010, **4**, 3647–3652.
14 A. D. Kuo, *Science*, 2005, **309**, 1686–1687; J. M. Donelan, Q. Li, V. Naing, J. A. Hoffer, D. J. Weber and A. D. Kuo, *Science*, 2008, **319**, 807–810; L. Moro and D. Benasciutti, *Smart Mater. Struct.*, 2010, **19**, 115011.
15 P. Calvert, *Nature*, 1975, **256**, 694; R. J. Gregorio, *J. Appl. Polym. Sci.*, 2005, **100**, 3272–3279.
16 T. T. Wang, H. von Seggern, J. E. West and H. D. Keith, *Ferroelectrics*, 1984, **61**, 249–256; T. Dargaville, M. Celina, J. Elliott, P. Chaplya, G. Jones, D. Mowery, R. Assink, R. Clough and J. Martin, Sandia Report (SAND2005–6846), Sandia National Laboratories, 2005; Y. Jiang, Y. Ye, J. Yu, Z. Wu, W. Li, J. Xu and G. Xie, *Polym. Eng. Sci.*, 2007, **47**, 1344–1350.
17 C. Chang, V. H. Tran, J. Wang, Y.-K. Fuh and L. Lin, *Nano Lett.*, 2010, **10**, 726–731.
18 S. Xu, Y. Qin, C. Xu, Y. Wei, R. Yang and Z. L. Wang, *Nat. Nanotechnol.*, 2010, **5**, 366–373.
19 G. Zhu, R. Yang, S. Wang and Z. L. Wang, *Nano Lett.*, 2010, **10**, 3151–3155.